

Learning Interpretable Characteristic Kernels via Decision Forests

Cencheng Shen

*Department of Applied Economics and Statistics
University of Delaware
Newark, DE 19716*

SHENC@UDEL.EDU

Sambit Panda

*Department of Biomedical Engineering and Institute of Computational Medicine
Johns Hopkins University
Baltimore, MD 21218*

SPANDA3@JHU.EDU

Joshua T. Vogelstein

*Department of Biomedical Engineering, Institute for Computational Medicine, Center for Imaging
Science, Kavli Neuroscience Discovery Institute
Johns Hopkins University
Baltimore, MD 21218*

JOVO@JHU.EDU

Editor:

Abstract

Decision forests are popular tools for classification and regression. These forests naturally produce proximity matrices measuring how often each pair of observations lies in the same leaf node. It has been demonstrated that these proximity matrices can be thought of as kernels, connecting the decision forest literature to the extensive kernel machine literature. While other kernels are known to have strong theoretical properties such as being characteristic, no similar result is available for any decision forest based kernel. In this manuscript, we prove that the decision forest induced proximity can be made characteristic, which can be used to yield a universally consistent statistic for testing independence. We demonstrate the performance of the induced kernel on a suite of 20 high-dimensional independence test settings. We also show how this learning kernel offers insights into relative feature importance. The decision forest induced kernel typically achieves substantially higher testing power than existing popular methods in statistical tests.

Keywords: Kernel Learning, Random Forest, Independence Testing, K -Sample testing

1. Introduction

Decision forests are ensemble method popularized by Breiman (2001, 2002). By random partitioning the feature set and constructing a multitude of decision trees via the training data, they perform very well for classification and regression problems, especially in high-dimensions (Caruana and Niculescu-Mizil, 2006; Caruana et al., 2008). A proximity matrix can then be used to measure how close two observation are in the partition. While there are many potential procedures for computing proximity from a forest, a popularly defined proximity for any two observations x_i and x_j is the percentage of trees for which both observations lie in the same leaf node. The proximity matrix can be thought of as an induced

similarity or kernel matrix from the decision forest. In general, any random partition algorithm may induce such a kernel matrix.

In this paper, we prove that the random forest induced kernel can be characteristic, and investigate its application for testing independence and two-sample testing where characteristic kernels play an important role. The traditional Pearson's correlation and its rank variants (Pearson, 1895; Spearman, 1904; Kendall, 1970) are still popular to detect linear and monotonic relationships when $p = q = 1$, but they are not consistent for detecting general relationships. The more recent distance correlation (Dcorr) (Székely et al., 2007; Székely and Rizzo, 2013) and the kernel correlation (HSIC) (Gretton et al., 2005, 2012a) are shown to be consistent for testing independence against any distribution of finite second moments at any finite p, q . In particular, a characteristic kernel plays a central role in achieving universal consistent testing for independence and two-sample testing (Sejdinovic et al., 2013; Lyons, 2013, 2018; Shen and Vogelstein, 2020).

One particular hurdle is the finite-sample testing power of these methods: despite being consistent and able to detect any relationship when the sample size is sufficiently large, the finite sample testing power may be low when the sample size is insufficient for the given dependency, such as strongly nonlinear dependency, too much noise in the relationship, and too high the dimensionality. In addition, choosing an appropriate kernel/metric that properly summarize complexities within the data is often times non-obvious (Sejdinovic et al., 2012). The high-dimensional data is a particularly vexing issue (Ramdas et al., 2015; Vogelstein et al., 2019), and a number of extensions have been proposed to achieve better power such as adaptive metric kernel choice (Gretton et al., 2012b), low-dimensional projections (Huang and Huo, 2017), marginal correlations (Shen, 2020), and some achieve better computational efficiency such as mondrian forests (Lakshminarayanan et al., 2014). In addition, interpretability is very desirable for hypothesis tests, but very few currently exist (Jitkrittum et al., 2016). As random forest is a very competitive learning method for high-dimensional data, we explore the properties of the random forest induced kernel for hypothesis testing, show that it can be made into a characteristic kernel, demonstrate its empirical advantage for high-dimensional data as a new test, kernel mean embedding random forest (KMERF), and demonstrate how it can elucidate relative feature importance to better interpret results..

2. Preliminaries

Hypothesis Testing

The testing independence hypothesis is formulated as follows: given paired sample data $\{(x_i, y_i) \in \mathbb{R}^{p+q}, i = 1, \dots, n\}$ where p denotes the dimension of x_i and q denotes the dimension of y_i , independence testing aims to test

$$\begin{aligned} H_0 &: F_{XY} = F_X F_Y, \\ H_A &: F_{XY} \neq F_X F_Y, \end{aligned}$$

by assuming $\{(x_i, y_i) \stackrel{iid}{\sim} F_{XY}\}$. We denote a kernel correlation as $c^n(\mathbf{X}, \mathbf{Y})$, where $\mathbf{X} = \{x_i\}$ and $\mathbf{Y} = \{y_i\}$. When the kernel choice is characteristic, $c^n(\mathbf{X}, \mathbf{Y}) \rightarrow 0$ if and only if \mathbf{X} and \mathbf{Y} are independent (Gretton et al., 2005).

The two-sample hypothesis is formulated as follows: given $\{u_i, i = 1, \dots, n_1\}$ and $\{v_j, j = 1, \dots, n_2\}$ one would like to test

$$\begin{aligned} H_0 &: F_U = F_V, \\ H_A &: F_U \neq F_V \end{aligned}$$

by assuming $\{u_i \stackrel{iid}{\sim} F_U\}$ and $\{v_j \stackrel{iid}{\sim} F_V\}$. By concatenating the two datasets and introducing an auxiliary random variable, two-sample testing can be equivalently tested by kernel correlation (Shen et al., 2020a).

Characteristic Kernel

Here we formally define characteristic kernel and its related properties.

Definition 1 *Given a separable metric space \mathcal{Z} , e.g., \mathcal{R}^p . A kernel function $k(\cdot, \cdot) : \mathcal{Z} \times \mathcal{Z} \rightarrow \mathcal{R}$ represents the similarity of two observations in \mathcal{Z} , and an $n \times n$ kernel matrix for $\{x_i \in \mathcal{Z}, i = 1, \dots, n\}$ is defined by $\mathbf{K}(i, j) = k(x_i, x_j)$.*

- A kernel $k(\cdot, \cdot) : \mathcal{Z} \times \mathcal{Z} \rightarrow \mathbb{R}$ is positive definite when for any $n \geq 2$, $x_1, \dots, x_n \in \mathcal{Z}$ and $a_1, \dots, a_n \in \mathbb{R}$, it holds that

$$\sum_{i,j=1}^n a_i a_j k(x_i, x_j) \geq 0.$$

- A characteristic kernel is a positive definite kernel with the following property: for any two random variables X_1 and X_2 with distributions F_{X_1} and F_{X_2} ,

$$E[k(\cdot, X_1)] = E[k(\cdot, X_2)] \text{ if and only if } F_{X_1} = F_{X_2}. \quad (1)$$

3. KMERF Test Statistic and P-Value

The KMERF test statistic is computed using the following algorithm:

1. Run random forest with m trees. Independent bootstrap samples of size $n_b \leq n$ are drawn to build a tree each time; each tree structure within the forest is denoted as $\phi_w \in \mathbf{P}$, $w \in \{1, \dots, m\}$; $\phi_w(x_i)$ denotes the partition assigned to x_i .
2. Calculate the proximity kernel:

$$\mathbf{K}_{ij}^X = \frac{1}{m} \sum_{w=1}^m [\mathbf{I}(\phi_w(x_i) = \phi_w(x_j))],$$

where $\mathbf{I}(\cdot)$ is the indicator function for how often two observations lie in the same partition.

3. Compute the induced kernel correlation: let

$$\mathbf{L}_{ij}^X = \begin{cases} \mathbf{K}_{ij}^X - \frac{1}{n-2} \sum_{t=1}^n \mathbf{K}_{it}^X - \frac{1}{n-2} \sum_{s=1}^n \mathbf{K}_{sj}^X + \frac{1}{(n-1)(n-2)} \sum_{s,t=1}^n \mathbf{K}_{st}^X & \text{when } i \neq j \\ 0 & \text{otherwise.} \end{cases}$$

Then let $\mathbf{K}^{\mathbf{Y}}$ be the Euclidean distance induced kernel, and similarly compute $\mathbf{L}^{\mathbf{Y}}$ from $\mathbf{K}^{\mathbf{Y}}$. The unbiased kernel correlation equals

$$c^n(\mathbf{X}, \mathbf{Y}) = \frac{1}{n(n-3)} \text{tr}(\mathbf{L}^{\mathbf{X}} \mathbf{L}^{\mathbf{Y}}).$$

In the simulation section we consider the standard supervised random forest with $m = 500$ for the first step, which is also applicable to the unsupervised version or other random forest variants (Blaser and Fryzlewicz, 2016; Athey et al., 2018; Tomita et al., 2020). In the second step we take the proximity matrix as the induced kernel. The third step computes a consistent correlation measure utilizing the kernels. Note that in the simulations, we use distance correlation. We found that utilizing the multiscale version of the kernel correlation (Vogelstein et al., 2019; Shen et al., 2020b), which is equivalent for linear relationships while being better for nonlinear relationships, produced similar results to using distance correlation, but substantially increased runtimes.

A hypothesis test using the above statistic can be implemented by a permutation test. Specifically, first compute a kernel on the observed $\{x_i\}$ and $\{y_i\}$. Then randomly permute the index of $\{y_i\}$, repeat the kernel generation process for $\{y_i\}$ for each permutation. This process involves training a new random forest for each permutation. Finally, compute the test statistic for each of the permutations. Then the p-value equals the percentage the permuted statistics that are larger than the observed statistic. The independence hypothesis is rejected when the p-value is less than a pre-set type 1 error level, say $\alpha = 0.05$. This is a common testing procedure used for nonparametric dependence measures, which correctly controls the type 1 error level (Good, 2005).

4. Theoretical Properties

Theorem 2 *The random forest induced kernel $\mathbf{K}^{\mathbf{X}}$ is always positive definite.*

Proof The kernel is positive definite because it is a summation of permuted block diagonal matrix, with ones in each block and zeros elsewhere (Davies and Ghahramani, 2014), i.e.,

$$\mathbf{K}^{\mathbf{X}} = \frac{1}{m} \sum_{w=1}^m Q B Q^T,$$

where Q is a permutation matrix, and B is a block diagonal matrix with each block representing the leaf node, and the sum is over all m trees in the forest. Each block matrix is positive definite and permutation does not change eigenvalues. As summation of positive definite matrices is still positive definite, $\mathbf{K}^{\mathbf{X}}$ is positive definite. For example, when each leaf node only contains one observation, B becomes the identity matrix. ■

Next we show the kernel can be characteristic, when the tree partition area converges to 0. A similar property is also used for proving classification consistency in k-nearest-neighbor (Devroye et al., 1996), and we shall denote $N(\phi_w) \in \mathbb{R}_{\geq 0}^{L_w}$ as the maximum area of each partition.

Two-Sample Test

Theorem 3 Suppose as $n \rightarrow \infty$, $N(\phi_w) \rightarrow 0$ for each tree $\phi_w \in \mathbf{P}$ and each observation x_i . Then the random forest induced kernel $\mathbf{K}^{\mathbf{X}}$ is asymptotically characteristic.

Proof It suffices to prove Equation 1. The forward implication is trivial. To prove the converse, it suffices to investigate $E[\mathbf{K}^{\mathbf{X}}(\cdot, X_1)] = E[\mathbf{K}^{\mathbf{X}}(\cdot, X_2)]$, or equivalently

$$E_{X_1} \left(\frac{1}{m} \sum_{w=1}^m [\mathbf{I}(\phi_w(X_1) = \phi_w(z))] \right) = E_{X_2} \left(\frac{1}{m} \sum_{w=1}^m [\mathbf{I}(\phi_w(X_2) = \phi_w(z))] \right)$$

for any observation z .

We first show the above equality occurs if and only if $\phi_w(X_1) \stackrel{D}{=} \phi_w(X_2)$. Once again, the forward implication is trivial. The converse can be shown by contradiction: without loss of generality, suppose there exists a leaf node region R such that $\phi_w(X_1) \in R$ with probability 0.4 while $\phi_w(X_2) \in R$ with probability 0.5. Then for any observation z always in R , $E[\mathbf{K}^{\mathbf{X}}(z, X_1)] = 0.4 \neq E[\mathbf{K}^{\mathbf{X}}(z, X_2)] = 0.5$, which is a contradiction.

Next we show $\phi_w(X_1) \stackrel{D}{=} \phi_w(X_2)$ if and only if $F_{X_1} = F_{X_2}$. The forward implication is again trivial. The converse is shown by contradiction. Suppose $F_{X_1} \neq F_{X_2}$. Without loss of generality, there always exists a neighborhood $N(x)$ such that $Prob(X_1 \in N(x)) = 0.1 \neq Prob(X_2 \in N(x)) = 0.2$. Now, because each tree partition area converges to 0, we can always make $N(x)$ small enough so that $\phi_w(N(x)) = R$ almost surely for some leaf node region R . Then $Prob(\phi_w(X_1) = R) = 0.1 \neq Prob(\phi_w(X_2) = R) = 0.2$. Thus $\phi_w(X_1) \stackrel{D}{\neq} \phi_w(X_2)$, contradiction.

Therefore, Equation 1 is proved, and the kernel is characteristic. ■

It follows from Gretton et al. (2005) that

Corollary 4 KMERF satisfies

$$c^n(\mathbf{X}, \mathbf{Y}) \xrightarrow{n \rightarrow \infty} c \geq 0,$$

with equality to 0 if and only if $F_{XY} = F_X F_Y$. Therefore the method is universally consistent for independence and two-sample testing.

5. Simulations

In this section we exhibit the consistency of KMERF, and compare its testing power with other competitors in a comprehensive simulation set-up. We utilize the `hyppo` package in Python (Panda et al., 2020), which uses `scikit-learn` random forest with 500 trees and default settings and calculate the proximity matrix from this. The KMERF is then computed via the kernel generation process in Section 3.

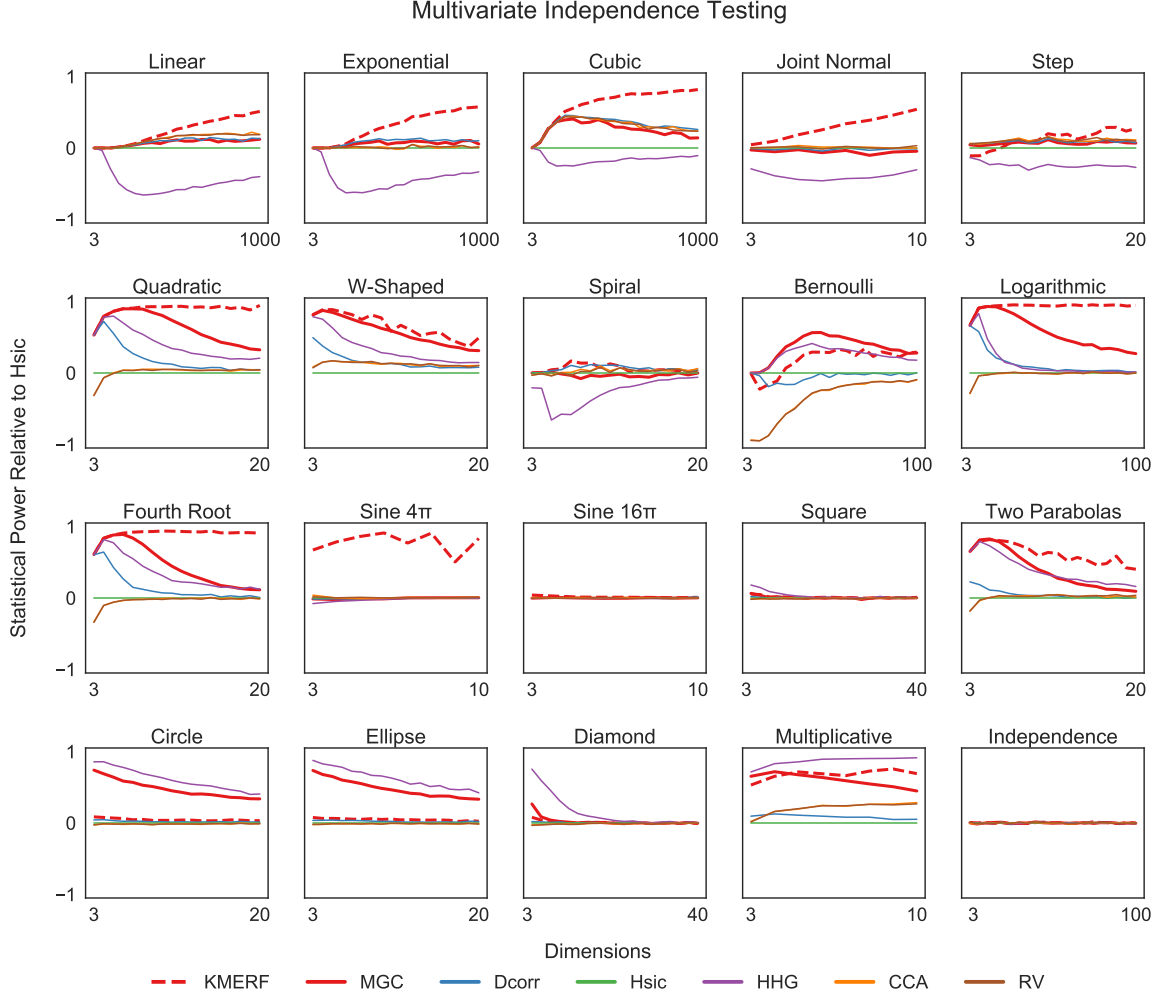


Figure 1: Multivariate independence testing power difference with respect to Hsic averaged over 5 repetitions for 20 different settings with increasing p , fixed $q = 1$, and $n = 100$. For the majority of the simulations, KMERF perm as well as, or better than, common multivariate independence tests in high-dimensional dependence testing.

Testing Independence

In this section we compare KMERF to the Multiscale Graph Correlation (MGC), Distance Correlation (Dcorr), Hilbert-Schmidt Independence Criterion (Hsic), and Heller-Heller-Gorfine (HHG) method, canonical correlation analysis (CCA), and RV coefficient. The HHG method is shown to work extremely well against nonlinear dependencies (Heller et al., 2013). The MGC method is shown to work well against linear, nonlinear, and high-dimensional dependencies (Shen et al., 2020b). The CCA and RV coefficients are popular

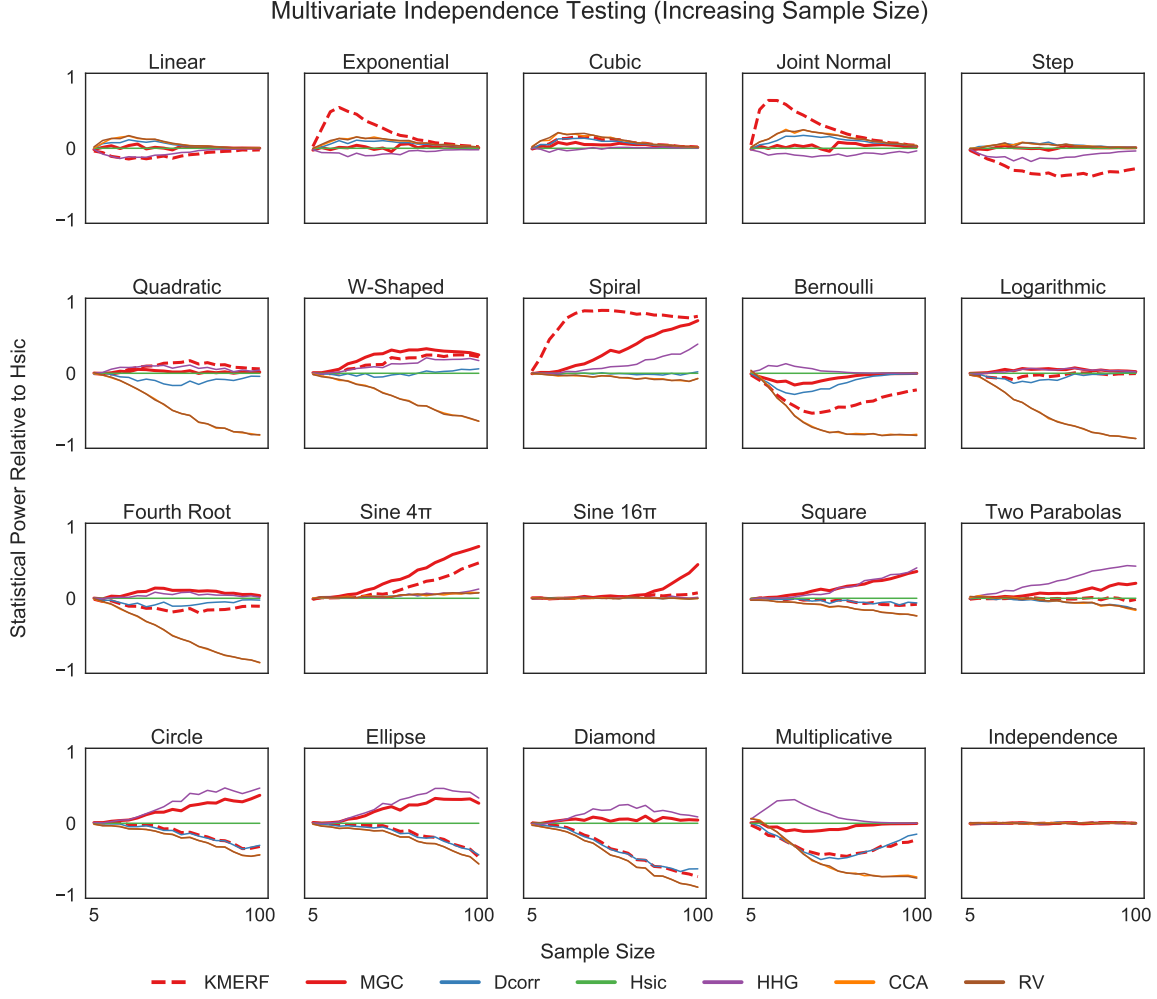


Figure 2: Multivariate independence testing power difference with respect to Hsic averaged over 5 repetitions for 20 different settings with increasing n , fixed $p = 5$ and $q = 1$. Once again, KMERF dominates all other tests in the majority of the simulation settings.

multivariate extension of Pearson correlation. For each method, we use the corresponding implementation in `hyppo` with default settings.

We take 20 high-dimensional simulation settings (Vogelstein et al., 2019) (the dependency details are available in the appendix), consisting of various linear, monotone and strongly nonlinear dependencies with p increasing, $q = 1$, and $n = 100$. To estimate the testing power in each setting, we generate dependent (x_i, y_i) for $i = 1, \dots, n$, compute the test statistic for each method, repeat for $r = 1000$ times; then we generate independent (x_i, y_i) for $i = 1, \dots, n$ using the same marginals, compute the test statistic for each method, and repeat for $r = 1000$ times. Via the empirical alternative and null distribution of the

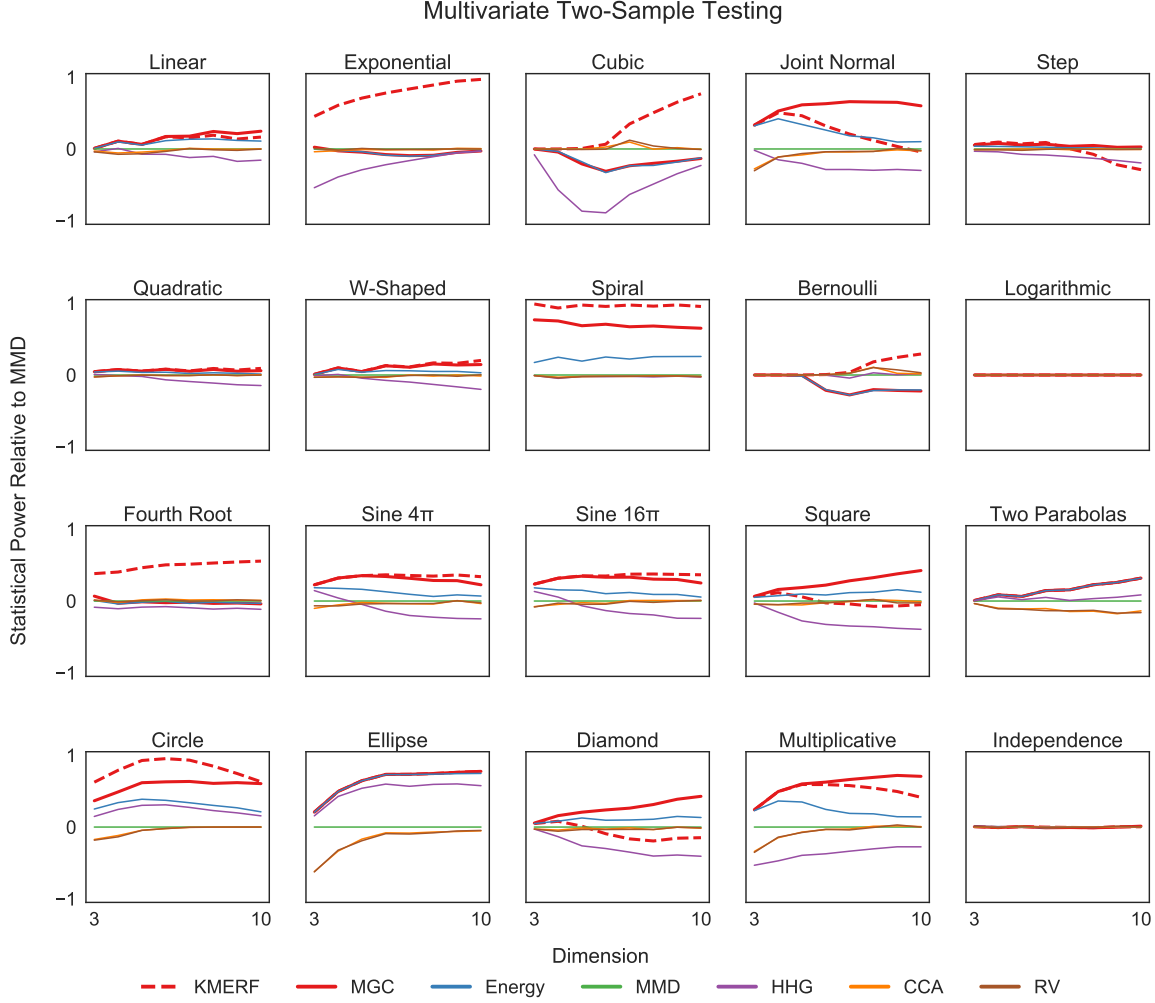


Figure 3: Multivariate two-sample testing power difference with respect to Hsic averaged over 5 repetitions for 20 different settings with increasing p , fixed $q = 1$, and $n = 100$. For the majority of the simulations, KMERF performs as well as, or better than, common multivariate two-sample tests in high-dimensional dependence testing.

test statistic, we estimate the testing power of each method at type 1 error level $\alpha = 0.05$, and take the average over five replications of this power calculation. The power result is shown in Figure 1 shows that KMERF achieves superior performance for most simulations, except a few functions like circle and ellipse.

We repeated the experiments in Figures 1, 3 to see the effects of increasing sample size at high dimensions for each tests as compared to Hsic (Figure 2). We see, in this case, that KMERF has higher statistical power compared to nearly every other test in these simulations settings.

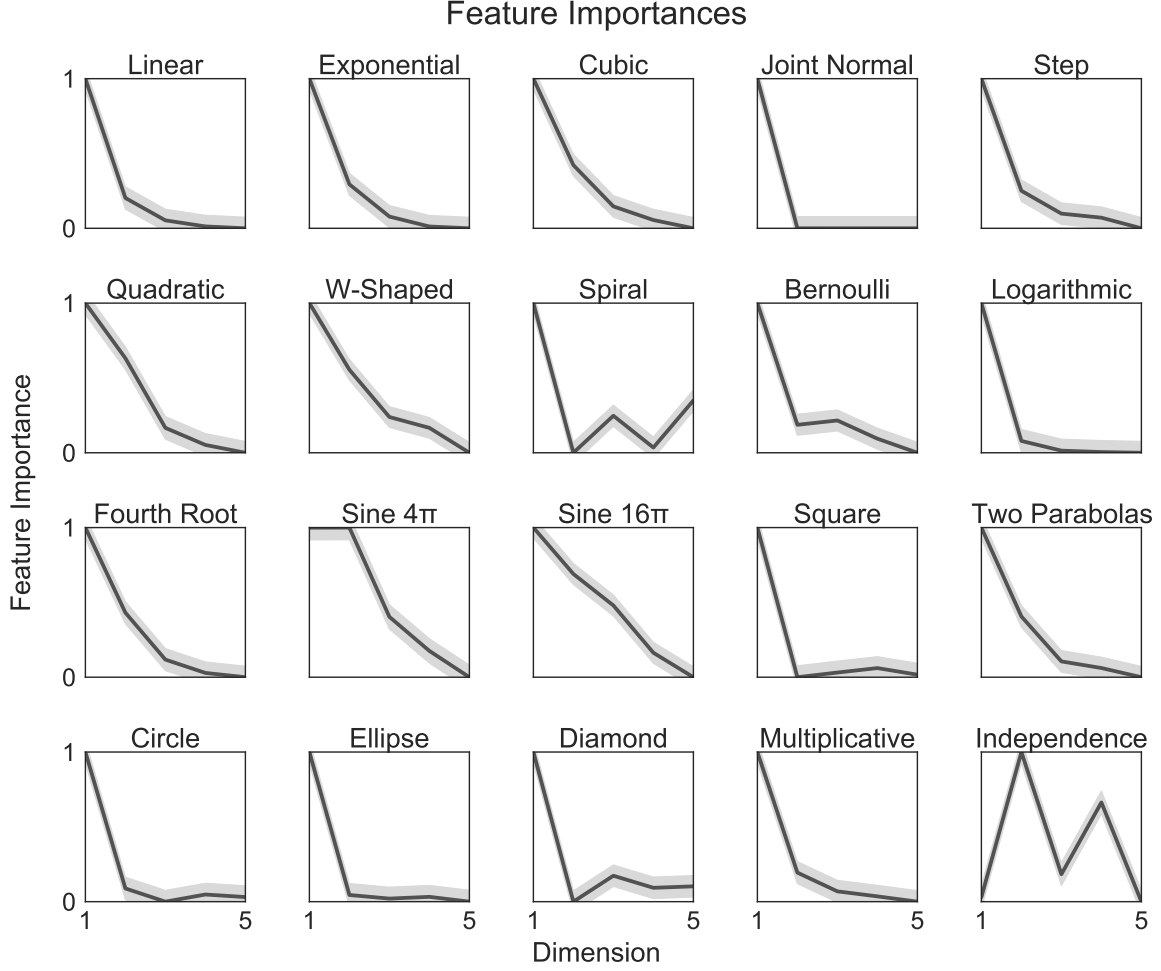


Figure 4: Normalized mean (black) and 95% confidence intervals (light grey) for relative feature importances derived from random forest over five dimensions for each simulation tested for 100 samples. A feature of KMERF is insights into interpretability, and we show here which dimensions of our simulations influence the outcome of independence test the most.

Two Sample Testing

Here, we compare the performance in the two-sample testing regime. It has been shown that all independence measures can be used for two-sample testing (Shen and Vogelstein, 2020), allowing all previous benchmark methods to be compared here as well. Once again, we investigate statistical power differences within 20 simulations settings consisting of various linear and nonlinear, monotonic and nonmonotonic functions with dimension increasing from $q = 1, \dots, 10$. We then apply a random rotation to this generated simulation to gen-

erate the second sample (via a rigid transformation). The function details are available in the appendix, and the testing process is same as before.

Figure 3 shows that, once again, for the majority of simulations settings, KMERF performs at or better than others especially when dimension increases. For certain simulation modalities, especially the exponential, cubic, and fourth root, KMERF vastly outperforms other metrics as dimensions increases. In some settings, KMERF performs worse at low dimensions, because performing random forest on single dimensional X is expected to be not effective.

5.1 Interpretability

Not only does KMERF offer better statistical power compared to alternatives, it offers insights into which features are the most important within the data set. Figure 4 shows normalised 95% confidence intervals of relative feature importances for each simulation, where the black line shows the normalized mean and the light grey line shows the 95% confidence interval. Within these simulations, we are able to determine that generally, feature importance decreases as dimension of the simulation increases, except for a few of the more complex simulations where this is not the case. The process we used to generate this figure can be trivially extended to a two-sample or k -sample case.

6. Real Data

KMERF performs better than alternatives in real data as well. We applied KMERF to a date set consisting of proteolytic peptides derived from the blood samples of 95 individuals harboring pancreatic ($n=10$), ovarian ($n=24$), colorectal cancer ($n=28$), and healthy controls ($n=33$). The processed data included 318 peptides derived from 121 proteins. Figure 5 shows the p-values for KMERF between pancreatic and healthy subjects compared to the p-values for KMERF between pancreatic and all other subjects. The test identifies neurogranin as a potentially valuable marker for pancreatic cancer, which the literature also corroborates (Yang et al., 2015; Willemse et al., 2018). Meanwhile, while some of the other tests identified this biomarker, it identified others that are upregulated in other types of cancers as well. We also show in the figure that the biomarker chosen be KMERF provides better true positive detection when compared to the other tests (there is no ground truth in this case, so a leave-one-out k -nearest-neighbor classification approach was used instead).

7. Discussion

KMERF is, to our knowledge, the first learned kernel that is proven to be characteristic. This is a first step towards building lifelong learning kernel machines with strong theoretical guarantees (Pentina and Ben-David, 2015; Vogelstein et al., 2020). The empirical experiments presented here illustrate the potential advantages of learning kernels even for static (rather than lifelong) learning problems, specifically under independence testing. The previously proposed approach for independence testing called MGC can be thought of, in a sense, as kernel learning: given n samples, and a pair of kernel or distance functions, it chooses one of the approximately n^2 sparsified kernels, by excluding all but the nearest

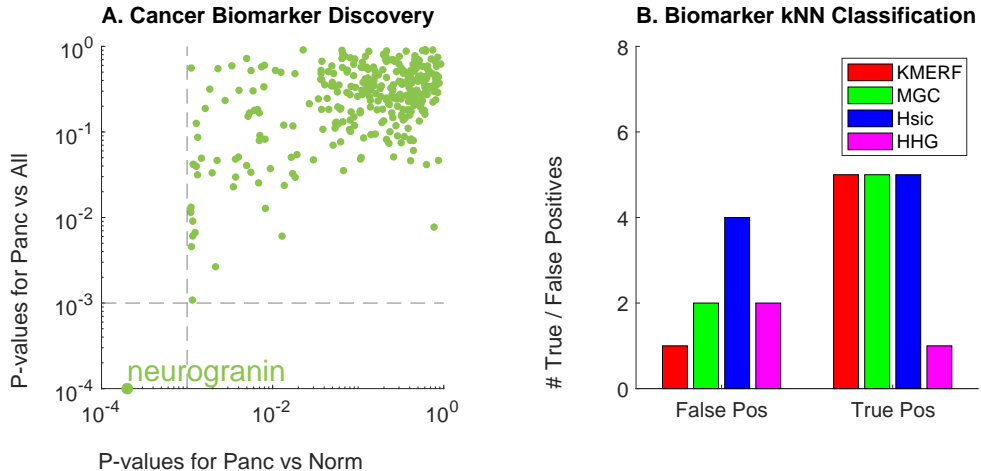


Figure 5: (A) For each peptide, the p-values for testing dependence between pancreatic and healthy subjects by KMERF is compared to the p-value for testing dependence between pancreatic and all other subjects. At the critical level 0.05, KMERF identifies a unique protein. (B) The true and false positive counts using a k -nearest neighbor (choosing the best $k \in [1, 10]$) leave-one-out classification using only the significant peptides identified by each method. The peptide identified by KMERF achieves the best true and false positive rates.

neighbors for each data point (Vogelstein et al., 2019; Shen et al., 2020b). Because RF can be thought of as a nearest neighbor algorithm (Lin and Jeon, 2006), in a sense, the RF induced kernel is a natural extension of that work, which leads to far more data-adaptive estimates of the nearest neighbors, using supervised information.

As the choice of kernel is crucial for empirical performance, this manuscript offers a new kernel construction that is not only universally consistent for testing independence, but also exhibits strong empirical advantage especially for high-dimensional testing. What is unique to this choice of kernel is the robustness and interpretability guarantees that are able to be ascertained when performing this test. It will be worthwhile to further understand the underlying theoretical mechanism of the induced characteristic kernel, as well as evaluating the performance of these RF induced kernels on other learning problems, including classification, regression, clustering, and embedding (Schölkopf and Smola, 2002).

Acknowledgments

This work is graciously supported by Microsoft Research, the Defense Advanced Research Projects Agency (DARPA) Lifelong Learning Machines program through contract FA8650-18-2-7834, the National Institute of Health awards R01MH120482 and T32GM119998, and the National Science Foundation award DMS-1921310.

Appendix A. Independence Simulation Functions

For the independence simulation, we test independence between X and Y . For the random variable $X \in \mathbb{R}^p$, we denote $X_{[d]}, d = 1, \dots, p$ as the d^{th} dimension of X . $w \in \mathbb{R}^p$ is a decaying vector with $w_{[d]} = 1/d$ for each d , such that $w^T X$ is a weighted summation of all dimensions of X . Furthermore, $\mathcal{U}(a, b)$ denotes the uniform distribution on the interval (a, b) , $\mathcal{B}(p)$ denotes the Bernoulli distribution with probability p , $\mathcal{N}(\mu, \Sigma)$ denotes the normal distribution with mean μ and covariance Σ , U and V represent some auxiliary random variables, κ is a scalar constant to control the noise level, and ϵ is sampled from an independent standard normal distribution unless mentioned otherwise.

1. **Linear**(X, Y) $\in \mathbb{R}^p \times \mathbb{R}$:

$$X \sim \mathcal{U}(-1, 1)^p,$$

$$Y = w^T X + \kappa\epsilon.$$

2. **Exponential**(X, Y) $\in \mathbb{R}^p \times \mathbb{R}$:

$$X \sim \mathcal{U}(0, 3)^p,$$

$$Y = \exp(w^T X) + 10\kappa\epsilon.$$

3. **Cubic**(X, Y) $\in \mathbb{R}^p \times \mathbb{R}$:

$$X \sim \mathcal{U}(-1, 1)^p,$$

$$Y = 128 \left(w^T X - \frac{1}{3} \right)^3 + 48 \left(w^T X - \frac{1}{3} \right)^2$$

$$- 12 \left(w^T X - \frac{1}{3} \right) + 80\kappa\epsilon.$$

4. **Joint Normal**(X, Y) $\in \mathbb{R}^p \times \mathbb{R}^p$: Let $\rho = 1/2p$, I_p be the identity matrix of size $p \times p$, J_p be the matrix of ones of size $p \times p$, and $\Sigma = \begin{bmatrix} I_p & \rho J_p \\ \rho J_p & (1 + 0.5\kappa) I_p \end{bmatrix}$. Then,

$$(X, Y) \sim \mathcal{N}(0, \Sigma).$$

5. **Step Function**(X, Y) $\in \mathbb{R}^p \times \mathbb{R}$:

$$X \sim \mathcal{U}(-1, 1)^p,$$

$$Y = \mathbb{I}(w^T X > 0) + \epsilon,$$

where \mathbb{I} is the indicator function; that is, $\mathbb{I}(z)$ is unity whenever z is true, and 0 otherwise.

6. **Quadratic**(X, Y) $\in \mathbb{R}^p \times \mathbb{R}$:

$$X \sim \mathcal{U}(-1, 1)^p,$$

$$Y = (w^T X)^2 + 0.5\kappa\epsilon.$$

7. **W-Shape**(X, Y) $\in \mathbb{R}^p \times \mathbb{R}$: For $U \sim \mathcal{U}(-1, 1)^p$,

$$X \sim \mathcal{U}(-1, 1)^p,$$

$$Y = 4 \left[\left(\left(w^\top X \right)^2 - \frac{1}{2} \right)^2 + \frac{w^\top U}{500} \right] + 0.5\kappa\epsilon.$$

8. **Spiral**(X, Y) $\in \mathbb{R}^p \times \mathbb{R}$: For $U \sim \mathcal{U}(0, 5)$, $\epsilon \sim \mathcal{N}(0, 1)$,

$$X_{|d|} = U \sin(\pi U) \cos^d(\pi U) \text{ for } d = 1, \dots, p-1,$$

$$X_{|p|} = U \cos^p(\pi U),$$

$$Y = U \sin(\pi U) + 0.4p\epsilon.$$

9. **Uncorrelated Bernoulli**(X, Y) $\in \mathbb{R}^p \times \mathbb{R}$: For $U \sim \mathcal{B}(0.5)$, $\epsilon_1 \sim \mathcal{N}(0, I_p)$, $\epsilon_2 \sim \mathcal{N}(0, 1)$,

$$X \sim \mathcal{B}(0.5)^p + 0.5\epsilon_1,$$

$$Y = (2U - 1) w^\top X + 0.5\epsilon_2.$$

10. **Logarithmic**(X, Y) $\in \mathbb{R}^p \times \mathbb{R}^p$: For $\epsilon \sim \mathcal{N}(0, I_p)$,

$$X \sim \mathcal{N}(0, I_p),$$

$$Y_{|d|} = 2 \log_2 (|X_{|d|}|) + 3\kappa\epsilon_{|d|} \text{ for } d = 1, \dots, p.$$

11. **Fourth Root**(X, Y) $\in \mathbb{R}^p \times \mathbb{R}$:

$$X \sim \mathcal{U}(-1, 1)^p,$$

$$Y = \left| w^\top X \right|^{1/4} + \frac{\kappa}{4}\epsilon.$$

12. **Sine Period 4 π** (X, Y) $\in \mathbb{R}^p \times \mathbb{R}^p$: For $U \sim \mathcal{U}(-1, 1)$, $V \sim \mathcal{N}(0, 1)^p$, $\theta = 4\pi$,

$$X_{|d|} = U + 0.02pV_{|d|} \text{ for } d = 1, \dots, p,$$

$$Y = \sin(\theta X) + \kappa\epsilon.$$

13. **Sine Period 16 π** (X, Y) $\in \mathbb{R}^p \times \mathbb{R}^p$: Same as above except $\theta = 16\pi$ and the noise on Y is changed to $0.5\kappa\epsilon$.

14. **Square**(X, Y) $\in \mathbb{R}^p \times \mathbb{R}^p$: For $U \sim \mathcal{U}(-1, 1)$, $V \sim \mathcal{U}(-1, 1)$, $\epsilon \sim \mathcal{N}(0, 1)^p$, $\theta = -\frac{\pi}{8}$,

$$X_{|d|} = U \cos(\theta) + V \sin(\theta) + 0.05p\epsilon_{|d|},$$

$$Y_{|d|} = -U \sin(\theta) + V \cos(\theta).$$

15. **Diamond**(X, Y) $\in \mathbb{R}^p \times \mathbb{R}^p$: Same as above except $\theta = \pi/4$.

16. **Two Parabolas** $(X, Y) \in \mathbb{R}^p \times \mathbb{R}$: For $\epsilon \sim \mathcal{U}(0, 1)$, $U \sim \mathcal{B}(0.5)$,

$$X \sim \mathcal{U}(-1, 1)^p,$$

$$Y = \left((w^\top X)^2 + 2\kappa\epsilon \right) \cdot \left(U - \frac{1}{2} \right).$$

17. **Circle** $(X, Y) \in \mathbb{R}^p \times \mathbb{R}$: For $U \sim \mathcal{U}(-1, 1)^p$, $\epsilon \sim \mathcal{N}(0, I_p)$, $r = 1$,

$$X_{|d|} = r \left(\sin(\pi U_{|d+1|}) \prod_{j=1}^d \cos(\pi U_{|j|}) + 0.4\epsilon_{|d|} \right)$$

for $d = 1, \dots, p-1$,

$$X_{|d|} = r \left(\prod_{j=1}^p \cos(\pi U_{|j|}) + 0.4\epsilon_{|p|} \right),$$

$$Y_{|d|} = \sin(\pi U_{|1|}).$$

18. **Ellipse** $(X, Y) \in \mathbb{R}^p \times \mathbb{R}^p$: Same as above except $r = 5$.

19. **Multiplicative Noise** $(x, y) \in \mathbb{R}^p \times \mathbb{R}^p$: $u \sim \mathcal{N}(0, I_p)$,

$$x \sim \mathcal{N}(0, I_p),$$

$$y_{|d|} = u_{|d|} x_{|d|} \text{ for } d = 1, \dots, p.$$

20. **Multimodal Independence** $(X, Y) \in \mathbb{R}^p \times \mathbb{R}$: For $U \sim \mathcal{N}(0, I_p)$, $V \sim \mathcal{N}(0, I_p)$, $U' \sim \mathcal{B}(0.5)^p$, $V' \sim \mathcal{B}(0.5)^p$,

$$X = U/3 + 2U' - 1,$$

$$Y = V/3 + 2V' - 1.$$

Appendix B. Two-Sample Simulation Function

We do two-sample testing between Z and Z' , generated as follows: let $Z = [X|Y]$ be the respective random variables from the independence simulation setup. Then define Q_θ as a rotation matrix for a given angle θ , i.e.,

$$Q_\theta = \begin{bmatrix} \cos \theta & 0 & \dots & -\sin \theta \\ 0 & 1 & \dots & 0 \\ \vdots & \vdots & \ddots & \vdots \\ \sin \theta & 0 & \dots & \cos \theta \end{bmatrix}$$

Then we let

$$Z' = Q_\theta Z^\top$$

be the rotated versions of Z .

References

Susan Athey, Julie Tibshirani, and Stefan Wager. Generalized random forests. *Annals of Statistics*, 47(2):1148–1178, 2018.

Rico Blaser and Piotr Fryzlewicz. Random rotation ensembles. *Journal of Machine Learning Research*, 17(4):1–26, 2016.

Leo Breiman. Random forests. *Machine Learning*, 4(1):5–32, October 2001.

Leo Breiman. Some infinity theory for predictor ensembles. *Journal of Combinatorial Theory, Series A*, 98:175–191, 2002.

Rich Caruana and Alexandru Niculescu-Mizil. An empirical comparison of supervised learning algorithms. In *Proceedings of the 23rd international conference on Machine learning*, pages 161–168. ACM, 2006.

Rich Caruana, Nikos Karampatziakis, and Ainur Yessenalina. An empirical evaluation of supervised learning in high dimensions. *Proceedings of the 25th International Conference on Machine Learning*, 2008.

Alex Davies and Zoubin Ghahramani. The random forest kernel and creating other kernels for big data from random partitions. *arXiv:1402.4293v1*, 2014.

Luc Devroye, László Györfi, and Gábor Lugosi. *A Probabilistic Theory of Pattern Recognition*. Springer, 1996.

Philip Good. *Permutation, Parametric, and Bootstrap Tests of Hypotheses*. Springer, 2005.

Arthur Gretton, Ralf Herbrich, Alexander Smola, Olivier Bousquet, and Bernhard Schölkopf. Kernel methods for measuring independence. *Journal of Machine Learning Research*, 6:2075–2129, 2005.

Arthur Gretton, Karsten M. Borgwardt, Malte J. Rasch, Bernhard Schölkopf, and Alexander Smola. A kernel two-sample test. *Journal of Machine Learning Research*, 13:723–773, 2012a.

Arthur Gretton, Dino Sejdinovic, Heiko Strathmann, Sivaraman Balakrishnan, Massimiliano M. Pontil, Kenji Fukumizu, and Bharath K. Sriperumbudur. Optimal kernel choice for large-scale two-sample tests. In *Advances in neural information processing systems 25*, pages 1205–1213, 2012b.

Ruth Heller, Yair Heller, and Malka Gorfine. A consistent multivariate test of association based on ranks of distances. *Biometrika*, 100(2):503–510, 2013.

Cheng Huang and Xiaoming Huo. A statistically and numerically efficient independence test based on random projections and distance covariance. *arXiv*, 2017.

Wittawat Jitkrittum, Zoltán Szabó, Kacper P Chwialkowski, and Arthur Gretton. Interpretable distribution features with maximum testing power. In *Advances in Neural Information Processing Systems*, pages 181–189, 2016.

Maurice G. Kendall. *Rank Correlation Methods*. London: Griffin, 1970.

Balaji Lakshminarayanan, Daniel M Roy, and Yee Whye Teh. Mondrian forests: Efficient online random forests. In *Advances in neural information processing systems*, pages 3140–3148, 2014.

Yi Lin and Yongho Jeon. Random forests and adaptive nearest neighbors. *J. Am. Stat. Assoc.*, 101(474):578–590, 2006.

Russell Lyons. Distance covariance in metric spaces. *Annals of Probability*, 41(5):3284–3305, 2013.

Russell Lyons. Errata to distance covariance in metric spaces. *Annals of Probability*, 46(4):2400–2405, 2018.

Sambit Panda, Satish Palaniappan, Junhao Xiong, Eric W. Bridgeford, Ronak Mehta, Cencheng Shen, and Joshua T. Vogelstein. hyppo: A comprehensive multivariate hypothesis testing python package, 2020.

Karl Pearson. Notes on regression and inheritance in the case of two parents. *Proceedings of the Royal Society of London*, 58:240–242, 1895.

Anastasia Pentina and Shai Ben-David. Multi-task and lifelong learning of kernels. In *Algorithmic Learning Theory*, pages 194–208. Springer International Publishing, 2015.

Aaditya Ramdas, Sashank J. Reddi, Barnabás Póczos, Aarti Singh, and Larry Wasserman. On the decreasing power of kernel and distance based nonparametric hypothesis tests in high dimensions. In *29th AAAI Conference on Artificial Intelligence*, 2015.

Bernhard Schölkopf and Alexander J Smola. *Learning with kernels: support vector machines, regularization, optimization, and beyond*. MIT press, 2002.

Dino Sejdinovic, Arthur Gretton, Bharath Sriperumbudur, and Kenji Fukumizu. Hypothesis testing using pairwise distances and associated kernels (with appendix). *arXiv preprint arXiv:1205.0411*, 2012.

Dino Sejdinovic, Bharath Sriperumbudur, Arthur Gretton, and Kenji Fukumizu. Equivalence of distance-based and rkhs-based statistics in hypothesis testing. *Annals of Statistics*, 41(5):2263–2291, 2013.

Cencheng Shen. High-dimensional independence testing and maximum marginal correlation. <https://arxiv.org/abs/2001.01095>, 2020.

Cencheng Shen and Joshua T. Vogelstein. The exact equivalence of distance and kernel methods in hypothesis testing. <https://arxiv.org/abs/1806.05514>, 2020.

Cencheng Shen, Carey E. Priebe, and Joshua T. Vogelstein. The exact equivalence of independence testing and two-sample testing. <https://arxiv.org/abs/1910.08883>, 2020a.

Cencheng Shen, Carey E. Priebe, and Joshua T. Vogelstein. From distance correlation to multiscale graph correlation. *Journal of the American Statistical Association*, 115(529): 280–291, 2020b.

Charles Spearman. The Proof and Measurement of Association between Two Things. *The American Journal of Psychology*, 15(1):72, 1904. ISSN 00029556. doi: 10.2307/1412159. URL <http://www.jstor.org/stable/1412159?origin=crossref>.

Gábor Székely and Maria L. Rizzo. The distance correlation t-test of independence in high dimension. *Journal of Multivariate Analysis*, 117:193–213, 2013.

Gábor Székely, Maria L. Rizzo, and Nail K. Bakirov. Measuring and testing independence by correlation of distances. *Annals of Statistics*, 35(6):2769–2794, 2007.

Tyler M. Tomita, James Browne, Cencheng Shen, Jaewon Chung, Jesse L. Patsolic, Benjamin Falk, Jason Yim, Carey E. Priebe, Randal Burns, Mauro Maggioni, and Joshua T. Vogelstein. Sparse projection oblique randomer forests. *Journal of Machine Learning Research*, 2020.

Joshua T. Vogelstein, Qing Wang, Erick W. Bridgeford, Carey E. Priebe, Mauro Maggioni, and Cencheng Shen. Discovering and deciphering relationships across disparate data modalities. *eLife*, 8:e41690, 2019.

Joshua T Vogelstein, Hayden S Helm, Ronak D Mehta, Jayanta Dey, Weiwei Yang, Bryan Tower, Will LeVine, Jonathan Larson, Chris White, and Carey E Priebe. A general approach to progressive learning. *arXiv preprint arXiv:2004.12908*, 2020.

Eline AJ Willemse, Ann De Vos, Elizabeth M Herries, Ulf Andreasson, Sebastiaan Engelborghs, Wiesje M Van Der Flier, Philip Scheltens, Dan Crimmins, Jack H Ladenson, Eugeen Vanmechelen, et al. Neurogranin as cerebrospinal fluid biomarker for alzheimer disease: an assay comparison study. *Clinical chemistry*, 64(6):927–937, 2018.

Jun Yang, Frederick K Korley, Min Dai, and Allen D Everett. Serum neurogranin measurement as a biomarker of acute traumatic brain injury. *Clinical biochemistry*, 48(13-14): 843–848, 2015.